

# UC Irvine

## UC Irvine Previously Published Works

### Title

Functionalization of Alginate with Extracellular Matrix Peptides Enhances Viability and Function of Encapsulated Porcine Islets

### Permalink

<https://escholarship.org/uc/item/98d2r51n>

### Journal

Advanced Healthcare Materials, 9(9)

### ISSN

2192-2640

### Authors

Medina, Juan D  
Alexander, Michael  
Hunckler, Michael D  
[et al.](#)

### Publication Date

2020-05-01

### DOI

10.1002/adhm.202000102

Peer reviewed



# HHS Public Access

Author manuscript

*Adv Healthc Mater.* Author manuscript; available in PMC 2020 October 30.

Published in final edited form as:

*Adv Healthc Mater.* 2020 May ; 9(9): e2000102. doi:10.1002/adhm.202000102.

## Functionalization of alginate with extracellular matrix peptides enhances viability and function of encapsulated porcine islets

**Juan D. Medina,**

Biomedical Engineering, Petit Institute for Bioengineering and Bioscience, Georgia Institute of Technology, 315 Ferst Drive, Atlanta, GA 30332

**Michael Alexander,**

Surgery, School of Medicine at UC Irvine, 333 City Boulevard West, Suite 1600, Orange, CA 92868

**Michael D. Hunckler,**

Mechanical Engineering, Petit Institute for Bioengineering and Bioscience, Georgia Institute of Technology, 315 Ferst Drive, Atlanta, GA 30332

**Marc A. Fernández-Yagüe,**

Mechanical Engineering, Petit Institute for Bioengineering and Bioscience, Georgia Institute of Technology, 315 Ferst Drive, Atlanta, GA 30332

**María M. Coronel,**

Mechanical Engineering, Petit Institute for Bioengineering and Bioscience, Georgia Institute of Technology, 315 Ferst Drive, Atlanta, GA 30332

**Alexandra M. Smink,**

Pathology and Medical Biology, University of Groningen, University Medical Center Groningen, Groningen, the Netherlands, 9713 GZ Groningen, Netherlands

**Jonathan R. Lakey,**

Surgery and Biomedical Engineering at UC Irvine, 333 City Boulevard West, Suite 1600, Orange, CA 92868

**Paul de Vos,**

Pathology and Medical Biology, University of Groningen, University Medical Center Groningen, Groningen, the Netherlands, 9713 GZ Groningen, Netherlands

**Andrés J. García**

Mechanical Engineering, Petit Institute for Bioengineering and Bioscience, Georgia Institute of Technology, 315 Ferst Drive, Atlanta, GA 30332

### Abstract

Translation of transplanted alginate-encapsulated pancreatic islets to treat type 1 diabetes has been hindered by inconsistent long-term efficacy. This loss of graft function can be partially attributed

---

Jonathan R. T. Lakey jlakey@hs.uci.edu; Paul de Vos p.de.vos@umcg.nl; Andrés J. García andres.garcia@me.gatech.edu.

Conflict of interest

The authors declare no conflict of interest.

to islet dysfunction associated with the destruction of extracellular matrix (ECM) interactions during the islet isolation process as well as immunosuppression-associated side effects. This study aims at recapitulating islet-ECM interactions by the direct functionalization of alginate with the ECM-derived peptides RGD, LRE, YIGSR, PDGEA, and PDSGR. Peptide functionalization was controlled in a concentration-dependent manner and its presentation was found to be homogeneous across the microcapsule environment. Pre-weaned porcine islets were encapsulated in peptide-functionalized alginate microcapsules, and those encapsulated in RGD-functionalized alginate displayed enhanced viability and glucose-stimulated insulin release. Effects were RGD-specific and not observed with its scrambled control RDG nor with LRE, YIGSR, PDGEA, and PDSGR. This study supports the sustained presentation of ECM-derived peptides in helping to maintain health of encapsulated pancreatic islets and may aid in prolonging longevity of encapsulated islet grafts.

## Keywords

Alginate; cell encapsulation; type 1 diabetes; islet

Cell encapsulation within hydrogels has been explored as a protective measure for preventing antigen recognition by direct cell-to-cell contact, and it has shown promise in enhancing the survival and therapeutic effects of transplanted cells for the treatment of chronic conditions such as inflammatory diseases, liver and kidney disease, degenerative bone diseases, and degenerative motor neuron disorders.<sup>[1–7]</sup> A prominent application of cellular encapsulation is the transplantation of alginate-encapsulated allogeneic pancreatic islets to reverse type 1 diabetes (T1D), a debilitating disease that arises from the autoimmune destruction of insulin-producing  $\beta$  cells of the pancreas.<sup>[8–12]</sup> Progress in clinical allogeneic islet transplantation has led to insulin independence in almost 50% of recipients at five years after transplantation.<sup>[13]</sup> Despite this greater success in islet transplantation, human donor shortages and life-long immunosuppression to prevent graft rejection have limited its widespread adoption as current immunosuppressive protocols make patients prone to infections, increase the risk of cardiovascular and metabolic diseases, and impair revascularization of transplanted islets.<sup>[14–16]</sup> To enhance islet survival, efforts have sought to reduce islet stress associated with isolation and hostile graft conditions.<sup>[13]</sup> Important islet-ECM interactions that have regulative effects on pancreatic islet survival, insulin secretion, proliferation, morphology preservation, including focal adhesion-mediated biochemical signaling, are lost throughout the isolation process.<sup>[18–22]</sup> To recapitulate ECM-cell interactions on encapsulated mammalian cells, researchers have covalently tethered adhesion receptor recognition sequences, such as integrin-binding peptides, to alginate.<sup>[23–25]</sup> As ECM interactions are essential for islet-cell function, we hypothesized that incorporation of cell adhesion binding motifs RGD, LRE, YIGSR, PDGEA, or PDSGR into the alginate microcapsule environment restores important ECM interactions and improves survival of islets.<sup>[26, 27]</sup>

In this study, we covalently tethered ECM peptide motifs onto alginate to prepare adhesive peptide-presenting alginate microcapsules for islet encapsulation. Covalent tethering was performed using an efficient two-step reaction in which alginate is oxidized by sodium *m*-

periodate and subsequently functionalized with peptides via reductive amination using the non-toxic reducing agent 2-picoline-borane complex. This reaction leads to the formation of a stable secondary amine that tethers alginate to the N-terminus of a peptide and allows for controlled presentation of the peptide in a manner that is dependent on the degree of alginate oxidation and input peptide concentration. Compared to the popularly used carbodiimide chemistry, this reaction allows for a greater degree of peptide tethering and does not result in N-acylurea binding to the alginate backbone nor formation of urea derivatives.<sup>[28]</sup>

Alginate was oxidized using sodium *m*-periodate to yield reduceable dialdehyde groups by the cleavage of vicinal hydroxyl groups on the alginate backbone as previously described.<sup>[18]</sup> To determine the degree of oxidation, an indicator solution was mixed with aliquots of oxidized alginate to measure the amount of unreacted sodium *m*-periodate using UV-vis absorption spectroscopy.<sup>[29]</sup> The oxidation reaction was efficient as residual sodium *m*-periodate was not detected in alginate oxidized to levels below 32% (Table 1). Residual sodium *m*-periodate detected in alginate oxidized to levels greater than 32% may be attributed to the formation of hemiacetals that can react with nearby alcohol groups, making them inaccessible for further oxidation.<sup>[28]</sup> Since oxidized alginate exhibits greater rotational freedom due to rupture of carbon-carbon bonds during the process of aldehyde formation, CaCl<sub>2</sub>-mediated ionic crosslinking of alginate is compromised with increasing degree of oxidation.<sup>[29]</sup> Indeed, we confirmed this by the inability to synthesize spherical microcapsules at alginate degrees of oxidation greater than 12%.

Oxidized alginate was subsequently functionalized with ECM peptide motifs (Table 2) using a reductive amination reaction that led to the formation of a stable secondary amine crosslink between oxidized residues and the primary amine at the N-terminus of the ECM peptide motif.<sup>[30–34]</sup> To determine the efficiency of functionalizing oxidized alginate with peptides, fluorescent dye-labeled RGD peptide was conjugated to alginate. However, the reducing conditions quenched FITC- and Cy-5-labeled RGD peptides and interfered with quantification. We subsequently used an RGD peptide covalently tethered to the polycyclic aromatic anthracenecarboxylic acid fluorophore, which we found could withstand reducing conditions without affecting its fluorescence properties.

Functionalization of alginate with RGD-(anthracenecarboxylic acid) required at least some degree of alginate oxidation and was found to increase with the degree of oxidation (Figure 1A). Furthermore, functionalization levels of alginate with RGD was strongly dependent on the input peptide concentration up to a saturating concentration, likely due to limited availability of reactive aldehydes at high peptide concentrations (Figure 1B). These results demonstrate that both the degree of oxidation and input peptide concentration are important parameters for controlling peptide tethering to alginate using this scheme. All subsequent experiments involved alginate oxidized to a degree of 8% as it allowed for peptide conjugation at a high density without impairing the fabrication of spherical microcapsules.

To confirm that the fluorescent tag on (anthracenecarboxylic acid)-RGD does not affect peptide conjugation, unmodified RGD and (anthracenecarboxylic acid)-RGD were simultaneously reacted with oxidized alginate in a one-to-one ratio. A decrease in fluorescence emission matching the ratio of labeled to unlabeled peptide confirmed that the

anthracenecarboxylic acid moiety did not affect conjugation of the peptide onto oxidized alginate (Figure 1C).

Microcapsules were fabricated and pancreatic islets were encapsulated within alginate-beads using electrostatic bead generating techniques.<sup>[35]</sup> Importantly, we were able to fabricate capsules that present RGD peptide homogeneously across the intracapsular environment (Figure 2). This ensures that covalently tethered peptides are readily available for binding to encapsulated islets, allowing for the reintroduction of ECM-cell adhesion interactions lost during the isolation process. To evaluate the effects of different ECM binding motifs, we encapsulated pre-weaned porcine islets in alginate capsules covalently presenting five different ECM binding motifs found in laminins, collagen, and fibronectin, among others.<sup>[29]</sup> We also tethered an RDG-scramble peptide with no adhesive activity to alginate to serve as a negative control along with islets encapsulated in unmodified alginate and unencapsulated islets. We chose pre-weaned Yorkshire piglets as our islet source because of their scalable potential, cost-effective isolation process, and superior *in vitro* viability when compared to that of adult porcine islets.<sup>[25, 36]</sup> We observed high encapsulation efficiency across all peptide-functionalized alginates with >99% of recovered islets being encapsulated and a low frequency (<15%) of empty capsules. Importantly, the encapsulation efficiency for peptide-functionalized alginates was equivalent to unmodified alginate and average capsule diameter did not differ significantly across peptide groups ( $513 \pm 50 \mu\text{m}$ ) and that of unmodified alginate ( $515 \pm 30 \mu\text{m}$ ). Porcine islets encapsulated in RGD-functionalized alginate exhibited higher viability when compared to those encapsulated in unmodified alginate and alginate modified with RDG and the adhesive peptides LRE, YIGSR, PDGEA, and PDSGR (Figure 3A and 3B). To screen for functional effects that presented ECM motifs had on encapsulated islets, we subjected them to a series of glucose challenges and evaluated their insulin secretion profile. All groups were tested together and each replicate's source of islets was biologically independent. We also included a challenge with a high concentration of glucose with the phosphodiesterase inhibitor 3-isobutyl-1-methylxanthine (IBMX) to induce cAMP-dependent insulin secretion.<sup>[37]</sup> Islets encapsulated in RGD-modified alginate exhibited significant differences in insulin released in the first low glucose challenge versus that released in a high glucose challenge (Figure 4). In contrast, islets encapsulated in unmodified alginate, RDG-functionalized alginate, and alginate functionalized with LRE, YIGSR, PDGEA, and PDSGR exhibited lower insulin secretion and there was limited glucose-stimulated insulin secretion. Interestingly, unencapsulated islets exhibited dysfunctional secretion profiles dissimilar to most of the encapsulated islets. We speculate that this may be due to mechanical support the capsule provides and helps maintain islet integrity following isolation, shipping, and culture stressors.<sup>[38]</sup> These observations show a trend towards enhanced viability of encapsulated pancreatic islets in the presence of covalently bound RGD. Thus, reintroduction of specific ECM interactions is of benefit for encapsulated islets; furthermore, because of the innate complexities of cell-ECM interactions, it may be possible that these effects are more pronounced with the collective incorporation of ECM-mimicking peptides.

Major limitations that have prevented islet transplantations from becoming more widespread include lifelong immunosuppression and massive islet cell death following transplantation. The aim of this study was to enhance islet viability and function via functionalization of

alginate capsules with ECM binding motifs to re-establish lost islet-ECM interactions that are critical for maintaining islet function and viability. It is likely that the most pronounced effects were observed using RGD-functionalized alginate because of the broad array of integrin-binding interactions that the RGD motif participates in and its presence in islet matrix components such as collagen, laminin, vitronectin, and nidogen/entactin.<sup>[38–41]</sup> Furthermore, the strategy used to functionalize alginate with RGD is easily controlled and allowed for the incorporation of other ECM binding motifs that may be more relevant to other cell therapy applications. This approach could ultimately address barriers currently limiting the broad application of allogeneic islet transplantation to treat T1D.

## Experimental Section

### Oxidation of alginate:

Intermediate-G alginate (ISP Alginate Ltd UK) was purified as previously described.<sup>[42]</sup> Alginate was dissolved to a concentration of 8.8 mg/mL in double deionized water (ddH<sub>2</sub>O) and propanol (10% v/v) was added. The solution was degassed with argon gas and cooled to 4°C. Sodium *m*-periodate in ddH<sub>2</sub>O (0.25 M) was degassed with argon and cooled to 4°C. Sodium *m*-periodate was added to the alginate solution, and the reaction was undertaken in subdued light at 4°C for 48h. An aliquot (100  $\mu$ L) was taken to determine the degree of oxidation and the remaining solution was ultracentrifuge filtered with ddH<sub>2</sub>O at 1500xg in 4°C. Oxidized alginate was then shell frozen and lyophilized with a Labconco Freeze Dry System.

To determine the degree of oxidation, an indicator solution was made by mixing equal volumes of KI (Sigma-Aldrich) (20% w/v) and soluble starch (Sigma-Aldrich) in DPBS (1% w/v). The previously mentioned 100  $\mu$ L aliquot was diluted with ddH<sub>2</sub>O (40 mL) and indicator solution (1.5 mL) was mixed with diluted solution (1.5 mL) and ddH<sub>2</sub>O (0.5 mL). Absorbance at 486 nm was recorded using a GE Ultrospec 2100 pro UV/Visible spectrophotometer and unreacted periodate concentration was calculated using a standard curve.

### Reductive amination of oxidized alginates:

Lyophilized oxidized alginate was dissolved in ddH<sub>2</sub>O to a concentration of 6.0 mg/mL; methanol was then added to a final concentration of 12% (v/v). A custom-synthesized peptide (GenScript) dissolved in ddH<sub>2</sub>O (0.05 M) is added to the desired final concentration. 2-picoline-borane complex in methanol (0.25 M) was then added to a final concentration of 25.0 mM and the pH was adjusted to 5.8. ddH<sub>2</sub>O was added to bring the oxidized alginate concentration to 3.0 mg/mL. The reaction vial was put to shake for 48h at room temperature and samples are subsequently dialyzed against NaCl (0.05 M) followed by centrifugal filtration with ddH<sub>2</sub>O. Dialyzed samples were then shell frozen and lyophilized.

### Peptide binding characterization:

A fluorescent (anthracenecarboxylic acid)-modified RGD was custom synthesized by Thermo Fisher Scientific and was conjugated to oxidized alginates as described above. Fluorescence emission of (anthracenecarboxylic acid) RGD-functionalized alginate was

recorded using a BioTek Synergy H4 Hybrid multimode plate reader (excitation at 350 nm and emission at 540 nm) to determine the density of incorporated peptide. (Anthracenecarboxylic acid)-RGD microcapsules were imaged using an inverted confocal microscope and spatial distribution of (anthracenecarboxylic acid)-RGD was quantified on z-stack images using Fiji imaging software.

#### **Porcine islet isolation:**

One- to two-week old pre-weaned Yorkshire pig islets were isolated under procedures approved by the University of California Irvine, Institutional Animal Care and Use Committee. Pancreata were procured and stored in cold HBSS (<1 hour). Pancreata were minced and digested with Collagenase Type V (Sigma-Aldrich) in a 37°C shaking water bath for 15 minutes. The enzymatic digestion was quenched with HBSS supplemented with 1% porcine serum (Gibco-Thermo Fisher Scientific) and digested tissues were filtered through a 500 µm metal mesh. Islets were then cultured in maturation media made up of Ham's F-12 medium (Corning), HEPES (Sigma-Aldrich), L-glutathione (Sigma-Aldrich), nicotinamide (Sigma-Aldrich), ITS+3 (Sigma-Aldrich), gentamycin sulfate (Corning), Trolox (Sigma-Aldrich), heparin (Sagent Pharmaceuticals), Pefabloc (Santa Cruz Biotechnology), L-glutamine(Alfa Aesar), medium 199 (Corning) and 10% porcine serum.

#### **Porcine islet shipment:**

Islets isolated at UCI were cultured in maturation media for three days and were then shipped to GT in a 1:1 ratio of maturation media and CMRL 1066 (Corning) with 100 µM Necrostatin-1 (Abcam). Upon arrival to GT, quality control in the form of live/dead viability (described below) was performed on an aliquot of the porcine islets. All other islets were allowed to recover for 24 hours in T-150 untreated suspension flasks in a 37°C, 5% CO<sub>2</sub> humidified incubator before encapsulation.

#### **Islet encapsulation:**

Modified alginate was dissolved in Ca<sup>2+</sup>-free Krebs ringer HEPES (30 mg/mL) and allowed to hydrolyze overnight. Hydrolyzed alginate was sterilized with a 0.2 µm filter and subsequently mixed with porcine islets (1,000 IEQ/mL). The alginate-islet mixture was infused into a Nisco electrostatically driven encapsulator with a Harvard Apparatus programmable syringe pump. Alginate microdroplets cross-linked in a 100 mM CaCl<sub>2</sub>, 10 mM HEPES, 2 mM KCl solution. The alginate capsules were cross-linked for 30 minutes and then suspended in porcine islet media to be incubated in a 37°C, 5% CO<sub>2</sub> incubator for 5 days.

#### **Glucose-stimulated insulin release:**

Encapsulated/unencapsulated islets were pre-incubated in Krebs-Ringer bicarbonate buffer (3 mM glucose) overnight. The islets were then subject to three subsequent incubations in low glucose concentration (3 mM), high glucose concentration (28 mM), a low glucose concentration (3 mM), and a final high glucose (28 mM) + IBMX. Incubation buffer was frozen after each incubation and islet DNA content was extracted after the final high glucose + IBMX incubation. Insulin was measured with a porcine insulin ELISA (Mercodia) and

DNA content was quantified using a Quant-iT PicoGreen double-strand assay kit (Invitrogen).

### Live-dead staining:

Encapsulated and bare islets were incubated with Calcein AM (2 mM) and ethidium-homodimer (4 mM) and visualized using an inverted confocal microscope. Viability was quantified by calculating the percentage of total projected area of an islet that stained positive for Calcein AM using Fiji imaging software

### Acknowledgements

The authors acknowledge JDRF (2-SRA-2018-523-S-B), NIH (U01 AI132817), and the Cell and Tissue Engineering NIH Biotechnology Training Grant (T32 GM-008433).

### References

- [1]. de Vos P, Lazarjani HA, Poncelet D, Faas MM; *Adv. Drug Deliv. Rev* 2014, 68, 15.
- [2]. Orive G, Hernandez RM, Gascon AR, Calafiore R, Chang TMS, de Vos P, Hortelano G, Hunkeler D, Lacik I, Shapiro AM, Pedraz JL; *Nat. Med* 2003, 9, 104. [PubMed: 12514721]
- [3]. Leijts M, Villafuertes E, Haeck J, Koevoet W, Fernandez-Gutierrez B, Hoogduijn M, Verhaar J, Bernsen M, van Buul G, van Osch G; *Eur. Cell. Mater* 2017, 33, 43. [PubMed: 28138954]
- [4]. Zhang Y, Chen X-M, Sun D-L; *Int. J. Artif. Organs* 2014, 37, 133. [PubMed: 24619896]
- [5]. Zhao X, Liu S, Yildirimer L, Zhao H, Ding R, Wang H, Cui W, Weitz D; *Adv. Funct. Mater* 2016, 26, 2809.
- [6]. Sagot Y; *Eur. J. Neurosci* 1995, 7, 1313. [PubMed: 7582105]
- [7]. Weaver JD, Headen DM, Coronel MM, Hunckler MD, Shirwan H, García AJ, *Am J Transplant* 2019, 19, 1315. [PubMed: 30378751]
- [8]. Roep BO, Arden SD, de Vries RRP, Hutton JC; *Nature* 1990, 345, 632. [PubMed: 2190098]
- [9]. Lipes MA, Rosenzweig A, Tan KN, Tanigawa G, Ladd D, Seigman JG, Eisenbarth GS; *Science* 1993, 259, 1165. [PubMed: 8267690]
- [10]. Hutchings P, Rosen H, O'Reilly L, Simpson E, Gordon S, Cooke A; *Nature* 1990, 348, 639. [PubMed: 2250718]
- [11]. Shapiro AMJ, Lakey JR, Ryan EA, Korbitt GS, Toth E, Warnock GL, Knetemeyer NM, Rajotte RV; *N. Engl. J. Med* 2000, 343, 230. [PubMed: 10911004]
- [12]. "CITR Tenth Annual Data Report [online report]." The Collaborative Islet Transplant Registry (CITR), 2017.
- [13]. Pepper AR, Bruni A, Shapiro AMJ, *Curr Opin Organ Transplant* 2018, 23, 428. [PubMed: 29847441]
- [14]. Desai NM, Goss JA, Deng S, Wolf BA, Markmann E, Palanjian M, Shock AP, Feliciano S, Brunicki FC, Barker CF, Naji A, Markmann JF; *Transplantation* 2003, 76, 1623. [PubMed: 14702535]
- [15]. Zhang N, Su D, Qu S, Tse T, Bottino R, Balamurugan AN, Xu J, Bromberg JS, Dong HH; *Diabetes* 2006, 55, 2429. [PubMed: 16936190]
- [16]. Salama AD, Womer KL, Sayegh MH; *J. Immunol* 2007, 178, 5419. [PubMed: 17442921]
- [17]. Barkai U, Rotem A, de Vos P; *World J Transplant.* 2016, 6, 69.
- [18]. Dalheim MØ, Vanacker J, Najmi MA, Aachmann FL, Strand BL, Christensen BE, *Biomaterials* 2016, 80, 146. [PubMed: 26708091]
- [19]. Beattie GM, Montgomery AMP, Lopez AD, Hao E, Perez B, Just ML, Lakey JRT, Hart ME, Hayek A; *Diabetes* 2002, 51, 3435. [PubMed: 12453897]
- [20]. Lucas-Clerc C, Massart C, Champion JP, Launois B, Nicol M, *Mol. Cell. Endocrinol* 1993, 94, 9. [PubMed: 8375579]



- [21]. Navarro-Alvarez N, Rivas-Carrillo JD, Soto-Gutierrez A, Yuasa T, Okitsu T, Noguchi H, Matsumoto S, Takei J, Tanaka N, Kobayashi N; Cell Transplant. 2008, 17, 111. [PubMed: 18468241]
- [22]. Wang R, J. Endocrinol 1999, 163, 181. [PubMed: 10556766]
- [23]. Fonseca KB, Bidarra SJ, Oliveira MJ, Granja PL, Barrias CC, Acta Biomater. 2011, 7, 1674. [PubMed: 21193068]
- [24]. Rowley JA, Madlambayan G, Mooney DJ, Biomaterials 1999, 20, 45. [PubMed: 9916770]
- [25]. Llacua A, de Haan BJ, Smink SA, de Vos P, J. Biomed. Mater. Res. A 2016, 104, 1788. [PubMed: 26990360]
- [26]. Yang F, Williams CG, Wang D, Lee H, Manson PN, Elisseeff J, Biomaterials 2005, 26, 5991. [PubMed: 15878198]
- [27]. Mann BK, Tsai AT, Scott-Burden T, and West JL, Biomaterials 1999, 20, 2281. [PubMed: 10614934]
- [28]. Sandvig I, Karstensen K, Rokstad AM, Achmann FL, Formo K, Sandvig A, Skjåk-Bræk G, Strand BL, J. Biomed. Mater. Res. A 2014, 103<sup>a</sup>, 896. [PubMed: 24668730]
- [29]. Gomez CG, Rinaudo M, Villar MA, Carbohydr. Polym 2007, 67, 296.
- [30]. Burgess BT, Myles JL, Dickinson RB, Ann Biomed Eng. 2000, 28, 110. [PubMed: 10645794]
- [31]. Boateng SY, Lateef SS, Mosley W, Hartman TJ, Hanley L, Russell B, Am J Physiol Cell Physiol 2004, 288.
- [32]. Gilbert M, Giachelli CM, Stayton PS, J. Biomed. Mater. Res 2003.
- [33]. Kleinman HK, Graf J, Iwamoto Y, Sasaki M, Schasteen CS, Yamada Y, Martin GR, Robey FA, Arc Biochem Biophys 1989.
- [34]. Weber LM, Hayda KN, Haskins K, Anseth KS, Biomaterials 2007, 28, 3004. [PubMed: 17391752]
- [35]. Klokk TI, Melvik JE, J. Microencapsul 2002, 19, 415. [PubMed: 12396380]
- [36]. Huettner N, Dargaville TT, Forget A, Trends Biotechnol 2018, 36, 372. [PubMed: 29422411]
- [37]. Vanderschelden R, Sathialingam M, Alexander M, Lakey JRT, Cell Transplant. 2019, 28, 967. [PubMed: 31037984]
- [38]. Siegel EG, Wollheim CB, Kikuchi M, Renold AE, Sharp GW, J. Clin Invest 1980, 65, 233. [PubMed: 6153182]
- [39]. Arifin DR, Manek S, Call E, Arepally A, Bulte JWM, Biomaterials 2012, 33, 4681. [PubMed: 22444642]
- [40]. Stendahl JC, Kaufman DB, Stupp SI, Cell Transplant. 2010, 18, 1.
- [41]. Cheng JYC, Raghunath M, Whitelock J, Poole-Warren L, Tissue Eng. Part B Rev 2011, 17.
- [42]. Paredes-Juarez GA, de Haan BJ, Faas MM, de Vos P, Materials 2014, 7, 2087. [PubMed: 28788557]

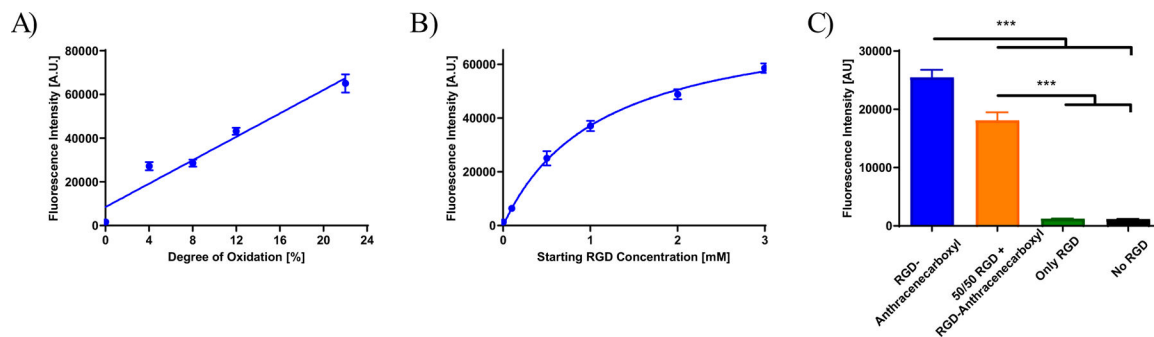


**Figure 1.** Fluorescence emission of (anthracenecarboxylic acid)-RGD-reacted alginates **A)** with varying oxidation degrees using a starting RGD concentration of 2.5 mM and **B)** varying initial peptide concentrations using alginate oxidized to a molar degree of 8%. **C)** Diminished fluorescence emission of (anthracenecarboxylic acid)-RGD in the presence of unmodified RGD (data presented as the average  $\pm$  standard deviation (n=3)). \*\*\*P<0.001; one-way ANOVA with Tukey multiple comparisons correction.

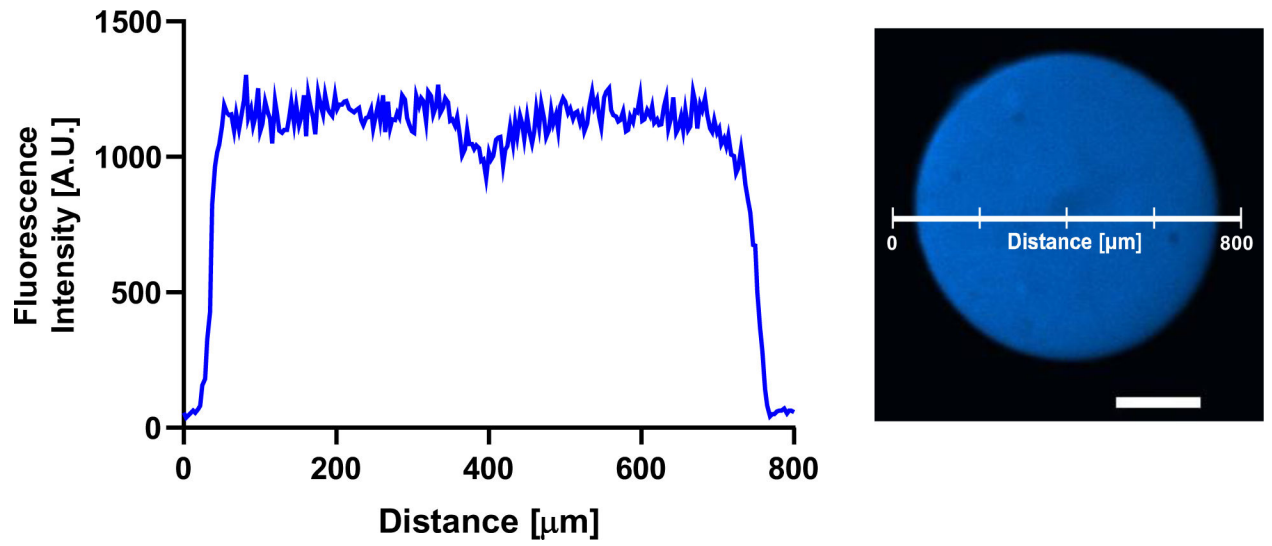


**Figure 2.** Fluorescence signal across a representative (anthracenecarboxylic-acid)-RGD-tagged alginate microcapsule (line across capsule indicates the spatial coordinates pertaining to the graph's y-axis; scale bar = 200  $\mu\text{m}$ ).

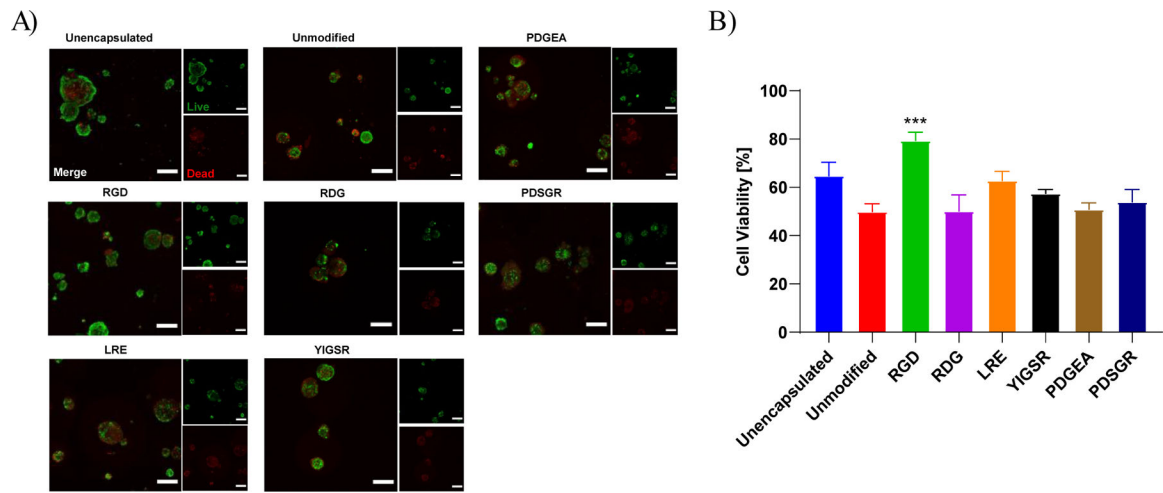


**Figure 3.**

**A)** Quality assessments of pre-weaned porcine islets encapsulated in different peptide-modified alginates by live-dead confocal imaging (scale bar = 200  $\mu$ m) **B)** Quantified cell viability (data presented as the mean  $\pm$  SD, n = 3 biologically independent samples).

\*\*\*P<0.001, nested one-way ANOVA with Dunnett's multiple comparisons test.

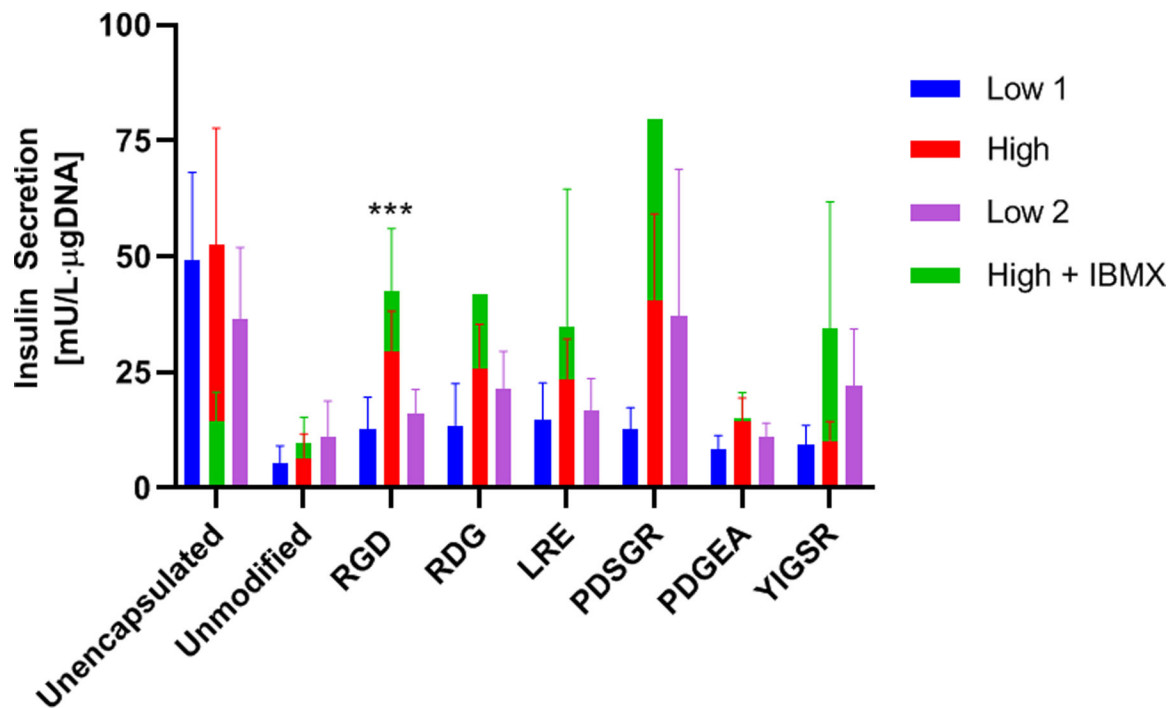


**Figure 4.** Functional assessment of islets by glucose-stimulated insulin response; \*\*\*P<0.001; nested t test for differences between insulin secretion at Low 1 vs High glucose challenge (data presented as the mean ± SEM (n = 4 biologically independent samples)).

**Table 1.**

Efficiency of oxidation of sodium alginate with sodium *m*-periodate at 4°C (data presented as the average ± standard deviation (n=3)).

| NaIO <sub>4</sub> Added [mol %] | NaIO <sub>4</sub> Reacted [mol %] |
|---------------------------------|-----------------------------------|
| 0                               | 0                                 |
| 4.0                             | $4.00 \pm 3.60 \times 10^{-3}$    |
| 8.0                             | $8.00 \pm 1.31 \times 10^{-3}$    |
| 12.0                            | $12.00 \pm 4.27 \times 10^{-4}$   |
| 32.0                            | $31.99 \pm 2.26 \times 10^{-4}$   |
| 64.0                            | $63.98 \pm 6.17 \times 10^{-5}$   |

Author Manuscript

Author Manuscript

Author Manuscript

Author Manuscript

**Table 2.**

Adhesive peptides used and their respective ECM proteins.

| Peptide Abbreviation | Peptide Sequence | ECM Protein(s)  |
|----------------------|------------------|---|
| RGD                  | GRGDSP           | Fibronectin, Vitronectin, Nidogen/Entactin, Laminin, Collagen |
| LRE                  | GLRE             | Laminin   |
| PDSGR                | GPDSGR           | Laminin   |
| PDGEA                | GPDGEA           | Collagen I  |
| YIGSR                | GYIGSR           | Laminin   |

Author Manuscript

Author Manuscript

Author Manuscript

Author Manuscript